Aurelia aurita Inspired Artificial Mesoglea

Article *in* Integrated Ferroelectrics · January 2013

DOI: 10.1080/10584587.2013.851591

CITATIONS
3

READS
150

6 authors, including:

Keyur Joshi
Virginia Polytechnic Institute and State University
14 PUBLICATIONS **154** CITATIONS
SEE PROFILE

Deepam Maurya
Virginia Polytechnic Institute and State University
126 PUBLICATIONS **1,301** CITATIONS
SEE PROFILE

John Blottman
United States Navy
34 PUBLICATIONS **275** CITATIONS
SEE PROFILE

S.Jeba Priya
Karunya University
530 PUBLICATIONS **10,144** CITATIONS
SEE PROFILE

Integrated Ferroelectrics, 148:53–66, 2013

ISSN: 1058-4587 print / 1607-8489 online
DOI: 10.1080/10584587.2013.851591

Aurelia aurita Inspired Artificial Mesoglea

KEYUR JOSHI,[1,2] ALEX VILLANUEVA,[1,2] COLIN SMITH,[1,2]
DEEPAM MAURYA,[1,2] JOHN BLOTTMAN,[3]
AND SHASHANK PRIYA[1,2,*]

[1]Center for Energy Harvesting Materials and Systems (CEHMS), Virginia Tech, Blacksburg, VA 24061, USA
[2]Bio-Inspired Materials and Devices Laboratory (BMDL), Virginia Tech, Blacksburg, VA 24061, USA
[3]Naval Undersea Warfare Center, Newport, RI 02841-1708, USA

In this preliminary study, we report the mechanical and dielectric properties of polyvinyl alcohol (PVA)-ferritin hydrogel. This material was found to exhibit close resemblance to Aurelia aurita *(jellyfish) mesoglea in terms of stiffness modulus and water content. Systematic experiments were conducted on natural jellyfish to identify its compression modulus a function of deformation. In compressive testing* Aurelia aurita *mesoglea was found to exhibit nonlinear modulus in the range of −10 kPa to 70 kPa depending upon the compressive strain (0–50% strain). The negative stiffness is an artifact of tensile force experienced by the specimen at the beginning of the test due to surface tension. PVA hydrogels with 60% water to dimethyl sulfoxide (DMSO) ratio without ferritin particle (H60) and PVA hydrogels with 80% water to DMSO ratio with ferritin particle (F80) provided a good alternative to natural jellyfish mesoglea exhibiting shear modulus of 33.06 Pa and 39.99 Pa respectively as compared to 4.75 Pa for* Aurelia aurita *mesoglea. This is a significantly better match compared to the 1041.67 Pa shear modulus of Ecoflex, a soft polymer material commonly used in biomimetic robotics. A Mooney Rivlin model suggests that H60 and F80 compositions are about 6.9 times and 8.4 times stiffer than natural* Aurelia aurtia *mesoglea whereas Ecoflex is 219 times as stiff. Nanocomposite hydrogel consisting of PVA matrix and ferritin nanoparticles were found to exhibit higher durability over regular PVA hydrogels and had more consistent properties due to increased cross-linking at ferritin nanoparticle sites. The ferritin nanoparticles were found to act as springs, increasing the modulus by increasing the surface area of the cross-linked polymer chains and disrupting long linear chain patterns of the polymer. Natural* Aurelia aurita *was found to have water content of 96.3% with a standard deviation of 0.57% as compared to 85% water content of PVA-ferritin hydrogels. Use of this material in the design of biomimetic unmanned underwater vehicles is expected to reduce the power consumption, increase swimming efficiency, and better replicate the rowing kinematics of naturally occurring* Aurelia aurita.

Keywords Mesoglea; nanoparticle; PVA; Ecoflex; stiffness; hydrogel; composite

I. Introduction

Unmanned underwater vehicles (UUVs) have long been in use but increasingly there has been an impetus on developing biomimetic robots that can surpass the performance

Received December 9, 2012; in final form August 25, 2013.
*Corresponding author. E-mail: spriya@vt.edu

and enhance the functionality of traditional vehicles. For example – a robotic jellyfish, inspired by the species *Aurelia aurita* was recently developed and characterized [1] to mimic the efficient propulsion modes of medusa swimming. Many of the soft robots, including jellyfish robot, being developed to date utilize standard engineering materials such as room temperature vulcanization (RTV) silicone to develop the body of the UUVs. RTV silicone is a good choice due to the low cost and the easy availability of a wide range of silicones. However, RTV silicones are not neutrally buoyant, are hydrophobic and too stiff to appropriately mimic the dynamic elastic properties of biological materials. There is critical need for creating artificial gel that can mimic the mechanical characteristics of soft flexible material such as jellyfish mesoglea. Deployment of biomimetic mesoglea instead of RTV silicone for robot body may significantly reduce the actuating force and therefore the power requirement of the vehicle. Multiple types of mesoglea exist within a given natural species: bell and joint, subumbrellar and exumbrellar. The objective of this paper is to design a nanocomposite hydrogel that mimics the mechanical properties of the natural *Aurelia aurita* bell mesoglea. In doing so, we developed and implemented a systematic methodology for measuring the mechanical properties of natural mesoglea.

II. Natural Mesoglea

Mesoglea makes up a majority of jellyfish volume [2]. It also provides structural support and helps in tailoring the kinematics of the animal. Mesoglea serves as the main locomotor surface such as the wing skin of a bat or the mantle of a squid. In achieving this additional functionality, it is evident that the mechanical properties of mesoglea play a special role. Thus, we have been making efforts towards understanding the dual role of mesoglea serving as both the structural and locomotor element. Mesoglea is a jelly-like substance comprised of long 20–50 nm diameter collagen fibers and a network of proteins and polysaccharides which span the space between the collagen fibers [3]. It is found in the taxa Cnidaria and Ctenophora but in this study we are primarily concerned with the jellyfish represented in the classes hydrozoa, scyphozoa, cubozoa, and staurozoa. The collagen fibers form a network which varies from one species to another. Chapman [4] has suggested that this network in *Aurelia aurita* is dense and random. It has interlinks with some cells interspersed in the mesoglea between the fibers. The collagen fibers for *Cyanea capillata* are sparse without many interlinks but are still random. *Chrysoara* species have relatively oriented and branched fibers. Collagen fibers provide the mesoglea with a large fraction of its elasticity and their arrangement determines the stiffness and other material properties of different parts of the jellyfish bell. The presence of varying collagen fiber network is the reason for jellyfish mesoglea exhibiting quite different elastic properties. Collagen fibers are made of three α chains of proteins. Polysaccharides and proteins act as food storage which is consumed by jellyfish during starvation. Mesoglea also has mucoprotein which takes part in digestion of food. Jellyfish mesoglea can be transparent, highly hydrophilic, neutrally buoyant, and possess low modulus while retaining durability [2]. These properties are partly due to the fact that mesoglea has such high water content, more than 96% [5].

The mechanical properties of mesoglea have scarcely been investigated. An attempt was made by Alexander [6] who studied viscoelastic properties of mesoglea and concluded that jellyfish (Scyphozoa, *Cyanea and Chrysaora*) mesoglea was softer than that of previously studied sea anemones (Anthozoa). Under deformation tests, mesoglea showed large

instantaneous strain and then a slow extension for long times (∼10 hr) before reaching a near-saturated state. This is in sharp contrast to the body-wall of sea anemones which have a very narrow distribution of retardation times. Gladfelter [7] has investigated the bell mesoglea of *Polyorchis montereyensis* as a rigid gel and the joint mesoglea as a much softer deformable gel that does not have viscoelastic properties. Demont and Gosline [8] found that intact jellyfish bell of the species *Polyorchis penicillatus* has a modulus between 400 and 1000 Pa. Megill et al. [9] found the stiffness of *Polyorchis penicillatus* bell mesoglea to be 350 Pa in compression while the softer joint mesoglea had stiffness of 50 Pa. Wang et al. investigated the mechanical properties of the jellyfish *Rhopilema esculenta Kishinouye* but did not report a single stiffness value [3]. Many of these prior studies indicate that the modulus of mesoglea varies over a wide range of magnitude. This could be associated with the measurement technique and also with the method of sample preparation. It is well-known that rapid changes in property of mesoglea occur as a function of time after it has been detached from the real animal. Gambini et al.'s [10] introduction of jellyfish extracellular material and micro-structures of the collagen fiber network provides insight into the structure of natural mesoglea. Zhu et al. [11] while studying the swelling properties and mechanical strength of natural mesoglea, developed an excellent method for SEM imaging of collagen network structures of the mesoglea.

The first objective in this paper is to quantify the bulk properties of natural jellyfish mesoglea to provide estimation for developing artificial materials. Based upon these measurements, the second objective is to successfully synthesize synthetic hydrogels that can replicate the mechanical performance of natural mesoglea. The rowing mechanism used by jellyfish for locomotion involves sequential contractions of the bell mesoglea. In this case, compressive modulus provides a reasonable metric for characterizing the performance because natural mesoglea is usually under a compressive load during this free-swimming [12].

III. Hydrogels as Candidate for Artificial Mesoglea

Much work has been done on synthetic hydrogels for a variety of purposes as diverse as tissue engineering [13], superabsorbent polymers [14], and gold ion reclamation into nanoparticles [15]. Hydrogels are an aqueous gel network composed typically of a hydrophilic polymer, cross-linked either by chemical bonds or cohesion forces. When placed in water, hydrogels are able to swell rapidly and retain large volumes of water without dissolving. Despite high water content, hydrogels are elastic solids that exhibit memory, a state to which the system can return after being deformed [16]. Conventional hydrogels are usually mechanically weak due to their lack of ordered structure at the molecular level [17]. However, recently there has been increasing progress in hydrogels with higher mechanical strength and robustness [18]. Wang et al. [3] have developed hybrid hydrogels based upon the mesoglea structure of the jellyfish *Rhopilema esculenta Kishinouye* but with the intent of achieving higher mechanical strength than other synthetic hydrogels. Hydrogels have been extensively evaluated by the medical field for their high fluid uptake, tunable stiffness and biocompatibility. They provide excellent solution for drug delivery, for absorption of large amount of body fluid in surgery and damaged tissue repair [19]. Conventionally hydrogels were seen as brittle materials with low stiffness, but recent advances in hydrogel research have made it possible to engineer them as flexible conducting material in seals and gaskets, as well as use them as cartilage to provide a robust shock-absorbing structure. Advances in durable hydrogels have opened the possibility of tailoring them for use in a biomimetic robotic jellyfish.

This class of material is highly tunable by way of nanofillers and can be synthesized by different methods including freeze-thaw, radiation, and chemical cross-linking agents. Naficy et al. [18] provide excellent review of prevalent robust hydrogel techniques. Nanocomposite (NC) gel consists of nanofillers in the primary polymer chains of hydrogel that act as cross-linking sites and improves the robustness of the gel. Single network (SN) gels are made up of long polymer chains with fewer cross-linking between them and are usually considered too brittle for engineering applications. Topological (TP) gel has slip links that hold two or more polymer links together but can slide along the link. TP gels can expand greatly on uptake of fluid and have excellent swelling and absorption characteristics. Double Network (DN) gels are more robust due to a highly cross-linked structure and are thus considered candidate materials in artificial cartilage. DN gels absorb large amount of shock and provide excellent stiffness characteristics. NC gels offer great flexibility in customization of gel properties by selection of the nanofillers, their amount and their distribution. Based upon this literature survey, we concluded that hydrogels serve as good starting point towards synthesizing artificial mesoglea. Tanaka et al.'s [20] review paper on different hydrogels with a special focus on techniques to improve mechanical performance was found to be particularly informative.

Nanofiller composites were found to be a viable option in increasing the strength due to their sustainability. In this study, ferritin was chosen as the candidate for nanofiller composite because of its structural uniformity on the nanoscale. With a protein shell of about 2 to 2.5 nm surrounding a ferritin-iron core of about 7 to 8 nm, the particles can form a network with polymer chains due to the carboxylic acid and the amino groups on the ferritin shells (see Figure 1). Nanofillers can decelerate crack propagation and delay complete failure of the composite hydrogel. Smaller filler particles increase surface area, which maximizes the interaction between the filler and polymer matrix. Ferritin exists naturally in a biocompatible form in various animals, plants, and bacteria for maintaining iron [21, 22]. Polymer nanocomposites based upon ferritin also have the possibility to respond to external stimuli and be mechanically adaptive. These properties could theoretically allow the body of the jellyfish to change stiffness, diffusion properties, or electrical conductivity [23].

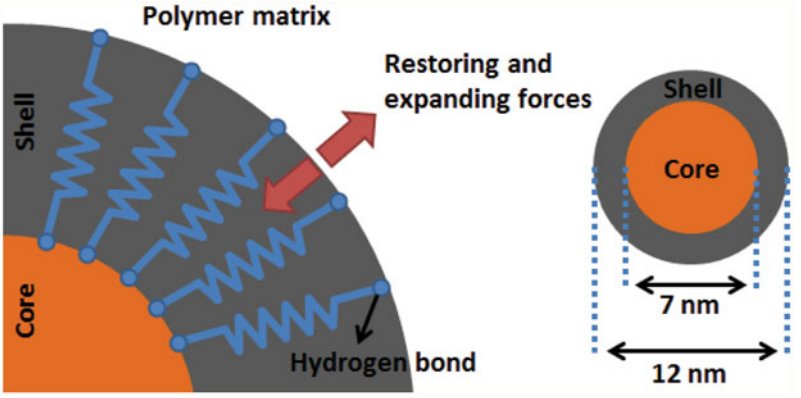

Figure 1. Elastic spring model of ferritin (protein) shell with ferritin (iron) core redrawn from Shin et al. [22] and 3D render of surface and cross-section of a ferritin nanoparticle redrawn from Ohara et al. [21]. (Color figure available online.)

IV. Synthesis and Characterization

A homogenous solution was prepared consisting of 15 wt% poly(vinyl alcohol) (PVA) with a molecular weight of ∼146,000 [24]. PVA was purchased from Sigma Aldrich (St. Louis, MO) and combined with a mixture of 18.2 MΩ-cm water and organic solvent dimethyl sulfoxide (DMSO). Mixing ratio of water to DMSO ranged from 50:50 to 90:10 by weight. DMSO with 99.9% purity (purchased from Sigma Aldrich) was thawed to room temperature liquid prior to use. Once PVA, water, and DMSO were combined, the solution was covered and stirred vigorously at 200°C for two hours. After sufficient mixing, the solution was a clear gel. The gel was swiftly poured into a mold, degased in a vacuum chamber, and then placed in a −5°C freezer for 10 hours to promote crystallization. The crystalized hydrogel was then placed in a flowing bath for 4 days, consisting of a constant supply of water to exchange DMSO in the gel with water [24].

Crystallinity has been found to increase with PVA concentration and freezing time, while the breakdown of crystalline structure was seen during the thawing process [17, 25]. Additionally, PVA polymer with higher molecular weight was chosen because it has been found to increase crystallite size and overall phase [26]. Upon further examination, it was found that the synthesized structure consisted of three phases: a water phase with low PVA concentration, an amorphous phase, and a crystalline phase that restricts some of the motion of the amorphous PVA chains. Researchers have introduced organic solvents during the freezing and thawing process to promote greater crystallinity [27]. This occurs because during the freezing stage the molecular movements are restricted. The intermolecular nucleation of PVA begins at this stage with the initiation of hydrogen bonding. With the addition of the organic solvent, crystallization can proceed further because of the lowered freezing temperature and significant volume expansion. This yields a much stronger and more durable hydrogel than conventional PVA synthesis [28].

IV.1 Preparation of PVA-Ferritin Nanocomposite Hydrogel

This material was synthesized by using the method described above for producing PVA hydrogel. However, prior to mixing water with PVA and DMSO, 0.25 grams of (10 mg/mL in 0.15 M NaCl) ferritin nanoparticles (purchased from Sigma Aldrich) was injected into 100 mL of 18.2 MΩ-cm water. The ferritin nanoparticle and water solution was sonicated for 5 minutes to ensure homogeneous dispersion. This mixture was then used in place of water in the standard PVA hydrogel preparation. PVA is a matrix for ferritin nanoparticles (FNPs) which are nanofillers. Other nanoparticles such as inorganic clays and carbon nanotube molecules have also been explored for improving the mechanical properties of hydrogels.

IV.2 Water Content of Natural **Aurelia aurita** *Jellyfish*

Five samples of approximately 22 mm diameter *Aurelia* jellyfish were lightly rinsed to remove excess salt water. The samples were then allowed to dry in air for 120 seconds to remove the surface water. The pre-dried weight was recorded and then the samples were exposed to light air flow under a fume hood for three days at which point the post-dry weight was recorded. After drying, salt crystals were observed on the samples, showing that the mesoglea was indeed carrying a large amount of sodium chloride from the surrounding seawater.

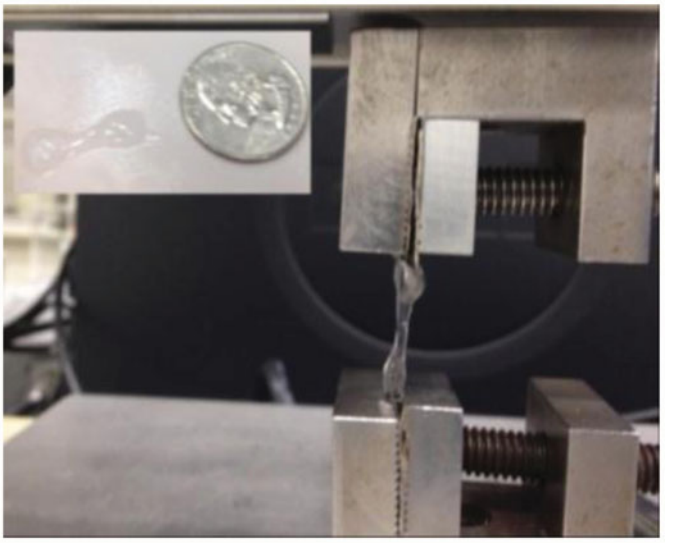

Figure 2. Texture analyzer setup for tensile testing of natural *Aurelia aurita* specimen. (Color figure available online.)

IV.3 Aurelia aurita *Mesoglea Testing*

A standard tension test was conducted on *Aurelia aurita* mesoglea using Texture Analyzer (TA.XTExpress) from Stable Microsystems Ltd. consisting of 5 kN load cell with 0.01 N resolution. Dogbone shapes were punched from live *Aurelia aurita* specimen of $\sim 3''$ diameter from the central region where bell has fairly uniform thickness as shown in the Fig. 2 inset. To avoid slipping, the specimen was placed between grit 80 sandpaper to provide grip. Some slip however was unavoidable due to visco-elastic nature of the mesoglea.

For compression testing, natural mesoglea was taken from *Aurelia aurita* specimens of around 30 mm in diameter. Rectangular samples of AACOMP1-21.9 $\times$ 24.36 $\times$ 3.67 mm^3, AACOMP2-13.4 $\times$ 24 $\times$ 3.94 mm^3 and AACOMP4-22.67 $\times$ 15.5 $\times$ 3.09 mm^3 were cut from the bell. Specimen AACOMP1 and AACOMP2 were taken from center of the bell, whereas AACOMP4 was taken towards flexible margin of the bell and possessed tapering thickness. The thickness was measured in air by digital calipers. All tests were conducted in an environment of 23 $\pm$ 2°C and 50 $\pm$ 6 % relative humidity. The same equipment and load cell were used to test both artificial and natural mesoglea. The test setup consisted of compression platens mounted on the moving end of the Texture Analyzer that pressed onto the specimen placed on waterproof sandpaper (grit 400) at the bottom to minimize the specimen slippage during compression. The compression platen was sufficiently larger than all the specimens to ensure uniform compression Specimens were compressed at a rate of 1 mm/min to $\sim$50% compressive strain.

IV.4 Compression Test of Artificial Mesoglea

For compression testing of hydrogel specimens, to give consistent results, a test method was developed by combining the guidelines from two existing ASTM standards that addresses compressive properties of rubbers and rigid plastics: ASTM D575 – Standard Test Methods

for Rubber Properties in Compression [29] and ASTM D695 – 10 Standard Test Method for Compressive Properties of Rigid Plastics [30]. These two standards were chosen as model methods because of the polymeric nature of PVA and the rubbery similarities that silicone exhibits.

PVA and PVA-ferritin hydrogels were compressed at a rate of 12.5 mm/min (0.5 ± 0.1 in/min) to achieve a deformation of 30% of the specimen thickness. The number 30% was chosen because naturally occurring *Aurelia aurita* has a maximum compressive deformation which does not exceed 30%. Specimens were cylindrical in shape with dimensions of 28.6 $\pm$ 0.1 mm in diameter and 12.5 ± 0.5 mm in thickness. All other test parameters are similar to natural mesoglea compression test.

V. Results and Discussion

V.1 Artificial Mesoglea Testing

PVA hydrogels exhibited non-linear behavior similar to that of the natural jellyfish mesoglea. There was a wide range of stiffness values, depending upon the water to DMSO ratio. Higher water to DMSO ratio lowered the stiffness of the material. The addition of FNPs was found to increase the stiffness of the hydrogel if the water to DMSO ratio was held constant. The addition of FNPs also eliminated the micro-failures in the hydrogel. Compression strength of PVA hydrogel and PVA ferritin nanocomposite hydrogel for various water to DMSO ratios is shown in Fig. 3(a) and (b). The different water to DMSO mix ratios such as 80% water and 20% DMSO is denoted as the percentage of water only ("80"). All strains are shown to 30% due to the maximum compression seen in jellyfish natural mesoglea.

V.2 **Aurelia aurita** *Mesoglea Testing*

The stress-strain behavior of natural *A. aurita* jellyfish mesoglea was found to be highly nonlinear, as displayed in Fig. 4. Due to this high degree of non-linearity, it is not possible to represent mesoglea stiffness in terms of a single value of Young's modulus. Due to the large amount of water present in the mesoglea, it exhibits a shape change under gravity and surface tension forces, as can be observed in Fig. 2. These difficulties due to the special nature of the mesoglea result in noisy data and the repeatability of the tensile test is compromised. The need for development of better tension testing method for mesoglea exists. Figure 5 illustrates the comparison of stress-strain behavior of Ecoflex-0010 Silicone, natural mesoglea samples and hydrogel samples that most closely matched to natural mesoglea in the compression test. Figure 5 suggests that H60 (PVA-hydrogel without Ferritin nanoparticles with 60:40 Water to DMSO ratio) and F80 (PVA-hydrogel with Ferritin nanoparticles with 80:20 Water to DMSO ratio) samples are initially equally as soft as natural mesoglea and match very closely to natural mesoglea stress-strain curve, but for high strains they deviate rapidly and becomes more stiff than natural mesoglea and the Ecoflex Silicone. Figure 6 represents tangent modulus $E(\epsilon) = \frac{d\sigma}{d\epsilon}$ as a function of strain for the AACOMP2 sample. The noise is a result of numerical differentiation with relatively small precision. The curve fit shows the representative trend in the change in tangent modulus with strain. The shape of the tangent modulus curve suggests that initially it increases but the rate of increase is reducing, reaching a fairly linear region near $\sim$0.25 strain and later increasing again at a rapid pace. This behavior is attributed to the material becoming softer after an initial hardening phase. At 15% strain, the tangent

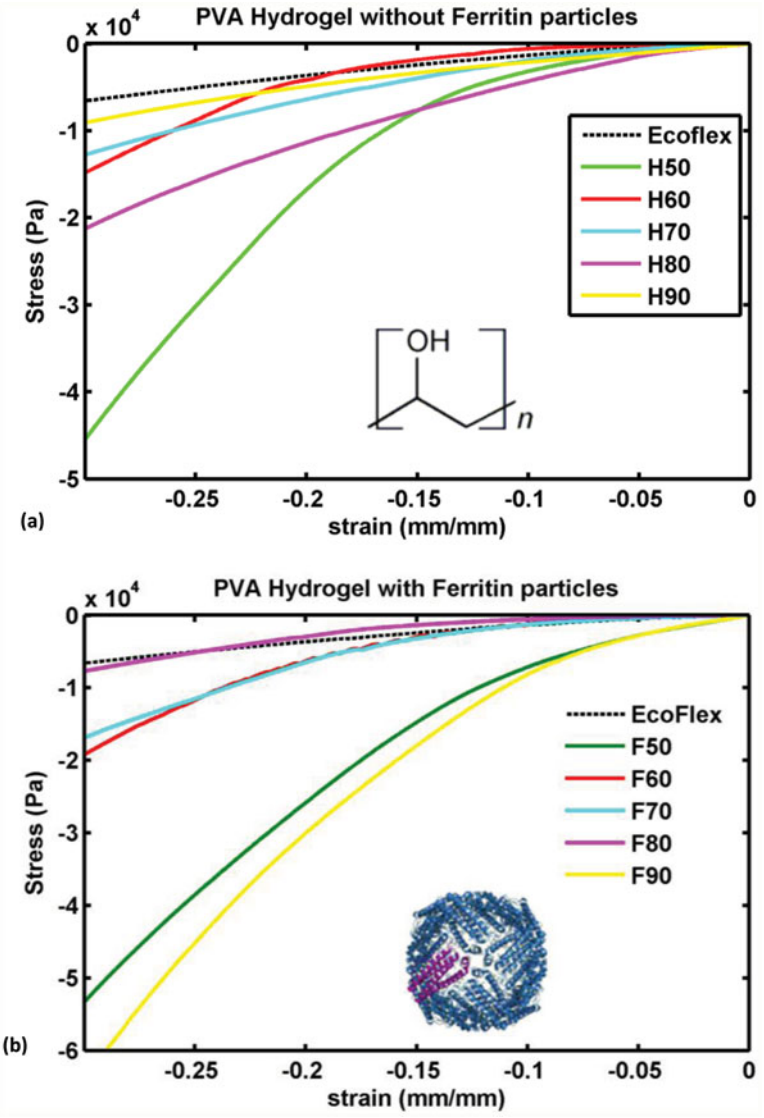

Figure 3. (a) Compression of PVA hydrogels of varying water content, (b) compression of PVA hydrogels of varying water content with ferritin nanoparticles, inset figure illustrates arrangement of polymer chains connected to a nanoparticle at the center.

modulus was 25 kPa, which is comparable with the results reported in the literature. Water was found to secrete out of the tissue during the experiment which may explain why there is a gradual increase in modulus. Finally, at large strains, the structure breaks down, reducing the mesoglea stiffness. This result is not shown in the figure. In comparison to the artificial mesoglea developed here (80:20 water/DMSO PVA hydrogel with ferritin particle), the tangent modulus at 15% strain was found to be ~8 kPa. According to the results from Villanueva et al. [31], the natural *Aurelia aurita* is expected to have a mesoglea compression of around 42% during a swimming cycle, however that actually refers to local bell diameter

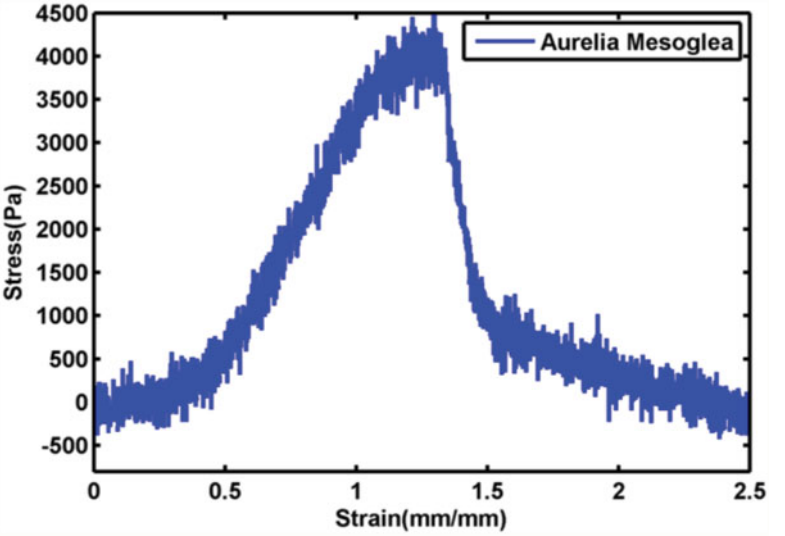

Figure 4. Stress-strain behavior of Aurelia aurita mesoglea in tension test. (Color figure available online.)

contraction, and does not necessarily mean the mesoglea is compressed 42%, rather quite smaller value of mesoglea contraction combined with geometric nonlinearity of the bell shape is sufficient to achieve this [32]. This measurement is relative to the bell diameter in the relaxed position. Water content in the *Aurelia* mesoglea was measured and was found to be 96.3% with a standard deviation of 0.57% as compared to the 90% water content of PVA-ferritin hydrogels.

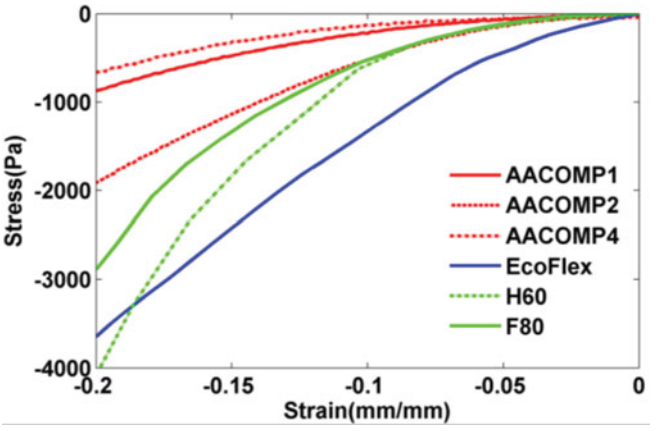

Figure 5. Stress-strain behavior of Aurelia aurita mesoglea in compression test in comparison with Ecoflex and closely matching hydrogel compositions H60 and F80. AACOMP1, AACOMP2 and AACOMP4 are compression test samples of Aurelia aurita mesoglea; Ecoflex is silicone rubber with shore hardness 0010 used as alternative to mesoglea in biomimetic robots, H60 is hydrogel sample without ferritin nanoparticle with 60–40 wt% water-DMSO mix, F80 is hydrogel sample with ferritin nanoparticle with 80–20 wt% water-DMSO mix.

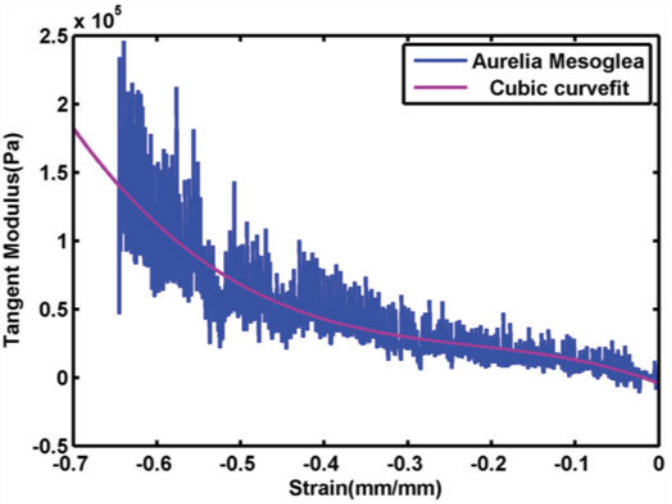

Figure 6. Tangent modulus of natural Aurelia aurita jellyfish mesoglea as a function of strain. (Color figure available online.)

V.3 Scanning Electron Microscope (SEM) Imaging

The microstructure of artificial mesoglea materials were studied using SEM to understand the change in the hydrogel structure caused by introduction of ferritin nanoparticles. The hydrogel samples were vacuum- dried to very high level (10^{-6} torr) and later sputtered with gold to increase its conductivity before SEM imaging. Figure 7(a) illustrates SEM of PVA-hydrogel without ferritin nano-particle with 70:30-Water/DSMO composition. The micro structure is wrinkly with lot of folds but has a regular linear pattern. These wrinkle or folds are caused by hydrogen bonds that create cross-links in long polymer chains and improve the elasticity of the material. Figure 7(b) illustrates the same material image but highlights the fault lines as observed in the hydrogel without ferritin nanoparticle. These fault lines break the regular linear pattern and are weak links in the hydrogel chains thus reducing material stiffness. Figure 7(c) illustrates SEM image of PVA-hydrogel with ferritin nanoparticle of the same composition. The addition of ferritin nanoparticles cause further wrinkles in the hydrogel patterns and now instead of a regular linear pattern, a randomly oriented short length mesh is observed. This is the result of additional hydrogen bonds formed around ferritin particles.

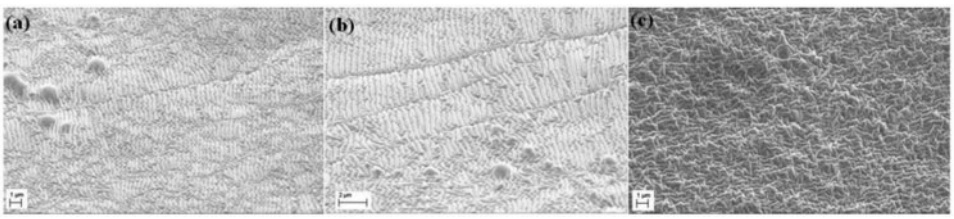

Figure 7. (a) PVA hydrogel without ferritin nanoparticles 70:30- Water:DSMO, (b) fault lines in PVA Hydrogel without ferritin nanoparticles 70:30- Water:DSMO and (c) PVA hydrogel with ferritin nanoparticles 70:30- Water:DSMO.

SEM imaging of natural mesoglea is particularly challenging due to the ∼96% water content and presence of a complex network of collagen fibers that make it impossible to remove all the water when air dried. Zhu et al. [11] have suggested freezing the mesoglea sample in liquid nitrogen to avoid formation of large water crystals that may damage the network structure. Accordingly, the jellyfish mesoglea samples were put in a container in liquid nitrogen to freeze them followed by vacuum-drying. The samples were then peeled off from the container wall, sputtered with gold and scanned under SEM. The collagen fiber network can be discerned from Fig. 8 (b), but the network has collapsed and the collagen fibers have coagulated into strands as seen in Fig. 8 (a). Also, due to incomplete desalination of the ocean water jellyfish, we can see some salt crystals trapped in the mesoglea (Fig. 8 (c)) that were not intended. Thus, although the SEM indicates the presence of a collagen fiber network, the fiber network structure could not be preserved.

V.4 Dielectric Constant

Samples of hydrogels with and without ferritin were characterized for their dielectric properties. Small samples of approximately 5.5 mm × 5.5 mm × 2 mm were cut from the larger blocks of hydrogel material. The small samples were allowed to dry in air for approximately 120 sec to allow excess surface moisture to evaporate. The hydrogel squares were then placed between two parallel copper plates, also of dimensions 5.5 mm × 5.5 mm. Care was taken to keep the copper plates in parallel with each other. A frequency sweep of capacitance was taken with an impedance analyzer (Hewlett Packard 4274A Multi-Frequency LCR Meter) from 500 Hz to 1 MHz. Figure 9(a) and (b) are the dielectric constants of PVA hydrogel with and without FNP reinforcement respectively over ∼500 kHz range. The dielectric constant for 90:10 PVA without FNPs was the highest while for PVA with FNPs 50:50 was the highest.

VI. Mooney Rivlin Model

Small deformation assumptions are no longer valid for modeling mesoglea material performance as the local coordinate system associated with the specimen is quite different as compared to the rigid global coordinate system. Thus, instead of defining the stress-strain relationship by Young's modulus in the usual sense that is coordinate system dependent, a hyperelastic material model that is capable of measuring strain independent of the coordinate system is needed. The standard method for representing elastic properties of hyperelastic materials is through non-linear models such as neo-hookean, Ogden or Mooney-Rivlin. We chose a 3-parameter Mooney Rivlin model to conduct comparative analysis of artificial

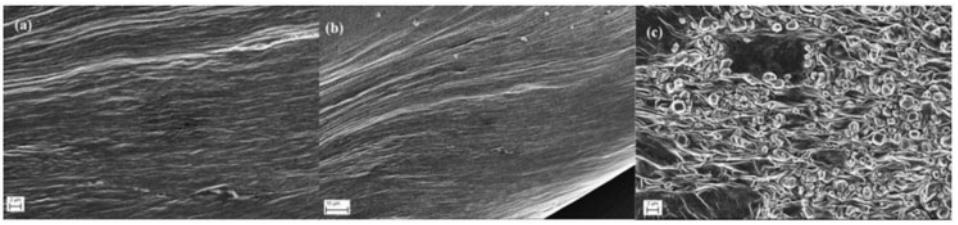

Figure 8. (a) Aurelia aurita mesoglea SEM image coagulated collagen fiber, (b) collapsed collagen fiber network, and (c) trapped salt crystals.

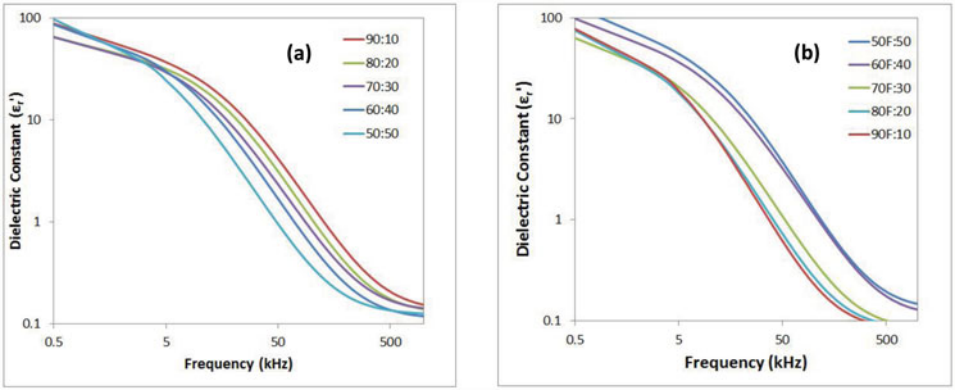

Figure 9. (a) Dielectric constants of PVA hydrogels, and (b) dielectric constant of PVA-ferritin nanocomposite hydrogels.

and natural mesoglea material. Equation (1) describes the strain energy density function W for the 3-parameter Mooney-Rivlin model, where, c_{10} is a measure of initial elastic modulus (slope of the stress-strain curve), d is the compressibility parameter, which is 0 for materials exhibiting incompressibility, $I_1 = \lambda_1^2 + \lambda_2^2 + \lambda_3^2$ and $I_2 = \frac{1}{\lambda_1^2} + \frac{1}{\lambda_2^2} + \frac{1}{\lambda_3^2}$ are strain invariants that remain independent of the co-ordinate system, $\lambda_1, \lambda_2, \lambda_3$ are stretches in any cartesian co-ordinate system, and J is the bulk deformation. For a two parameter model, $G = \frac{c_{10}+c_{01}}{2}$ is the shear modulus, but for higher order models, c_{mn} are just coefficients of m powers of $(I_1 - 3)$ and n powers of $(I_2 - 3)$. Table 1 compares the EcoFlex silicone model parameters taken from Joshi et al. [33] with that of natural mesoglea and candidate hydrogel materials for artificial mesoglea. Shear modulus calculated from the model provides a good basis for comparison of material stiffness irrespective of co-ordinate system.

$$W = c_{10}(I_1 - 3) + c_{01}(I_2 - 3) + c_{11}(I_1 - 3)(I_2 - 3) + \frac{1}{d}(J - 1)^2 \tag{1}$$

The coefficients of the model were calculated using ANSYS workbench tool that curve-fits eq. (1) through experimental stress-strain data to yield minimum residual to arrive at the coefficients. We recommend using shear modulus derived from Mooney-Rivlin coefficients

Table 1
Mooney-Rivlin parameters for Ecoflex silicone and *Aurelia aurita* mesoglea

Parameter	*Aurelia aurita* mesoglea	EcoFlex silicone	PVA Hydrogel without Ferritin nanoparticle (60:40 = Water/DMSO)	PVA Hydrogel with Ferritin nanoparticle (80:20 = Water/DMSO)
c_{10}	$-649.26Pa$	$2307.1Pa$	$69.398Pa$	$-781.86Pa$
c_{01}	$658.76Pa$	$-223.76Pa$	$-3.2453Pa$	$861.84Pa$
c_{11}	$474.66Pa$	$142.83Pa$	$2547.7Pa$	$1490.4Pa$
d	$0Pa^{-1}$	$0Pa^{-1}$	$0Pa^{-1}$	$0Pa^{-1}$
Shear modulus G	$4.75Pa$	$1041.67Pa$	$33.076Pa$	$39.99Pa$

as a basis of comparison for hyperelastic material. The comparison suggests that *A. aurita* mesoglea is about 7.8 times softer than Ecoflex. PVA hydrogel with ferritin nanoparticles (80% water -20% DMSO solution) was 5.8 times stiffer by comparing c_{10} and thus a better material for artificial mesoglea.

VII. Summary

A PVA based hydrogel is a promising base material for artificial mesoglea. Mechanical similarities exist between the PVA hydrogel reinforced with FNPs (nanofiller that act like elastic nanosprings) and biological mesoglea (a fiber reinforced tissue). Softer sections of joint mesoglea can be replicated by varying DMSO and nanofiller content to allow for folding during rowing contraction, which is seen in rowing jellyfish. Modulus pairing between artificial and natural mesoglea for specific regions is a potential topic of future research. Additionally, saltwater stability and absorption must be addressed to ensure that the outer layer does not degrade during use. The Mooney Rivlin model suggests that PVA hydrogel with ferritin nanoparticles (80% water-20% DMSO mix) and PVA hydrogel without ferritin nanoparticles (60% water-40% DMSO mix) provide good match with natural mesoglea material behavior for up to 10–15% strain where shear modulus values of 39.99Pa and 33.07Pa respectively are computed, compared to 4.75Pa for natural *Aurelia aurita* mesoglea, while traditionally used Ecoflex-0010 silicone is much stiffer with shear modulus 1041.67Pa.

Acknowledgments

This work is sponsored by the Office of Naval Research through contract number N00014-08-1-0654 Jellyfish Autonomous Node and Colonies MURI and the U.S. Army Research Office under grant number W911NF-07-1-0452 Ionic Liquids in Electro-Active Devices (ILEAD) MURI.

References

1. A. Villanueva, C. Smith, and S. Priya, "A biomimetic robotic jellyfish (Robojelly) actuated by shape memory alloy composite actuators," *Bioinspiration & Biomimetics* **6**, Sep (2011).
2. M. N. Arai, *Functional biology of Scyphozoa*: Springer, (1996).
3. X. Wang, H. Wang, and H. R. Brown, "Jellyfish gel and its hybrid hydrogels with high mechanical strength," *Soft Matter* **7**, 211–219, (2011).
4. G. Chapman, "Studies of the Mesogloea of Coelenterates: I. Histology and Chemical Properties," *Quarterly Journal of Microscopical Science* **s3–94**, 155–176, June 1, (1953).
5. Lowndes, "Percentage of Water in Jelly-Fish," *Nature (London)* **150**, 234–235, (1942).
6. R. McN. Alexander, "Visco-Elastic Properties of the Mesogloea of Jellyfish," *Journal of experimental Biology* **41**, 363–369, June 1, (1964).
7. W. G. Gladfelter, "Structure and function of the locomotory system of Polyorchis montereyensis (Cnidaria, Hydrozoa)," *Helgol. Wiss. Meeresunters.* **23**, 38, (1972).
8. M. E. Demont and J. M. Gosline, "Mechanics of Jet Propulsion in the Hydromedusan Jellyfish, Polyorchis Pexicillatus: I. Mechanical Properties of the Locomotor Structure," *Journal of experimental Biology* **134**, 313–332, January 1, (1988).
9. W. M. Megill, J. M. Gosline, and R. W. Blake, "The modulus of elasticity of the fibrillin-containing microfibrils from the mesoglea of the hydromedusa: polyorchis penicillatus," *J. Exp. Biol.* **208**, 3819, (2005).
10. C. Gambini, B. Abou, A. Ponton, and Annemiek J. M. Cornelissen, "Micro- and Macrorheology of Jellyfish Extracellular Matrix," *Biophysical Journal* **102**, 1–9, (2012).

11. J. Zhu, X. Wang, C. He, and H. Wang, "Mechanical properties, anisotropic swelling behaviours and structures of jellyfish mesogloea," *Journal of the Mechanical Behavior of Biomedical Materials* **6**, 63–73, (2012).
12. J. O. Dabiri, S. P. Colin, and J. H. Costello, "Fast-swimming hydromedusae exploit velar kinematics to form an optimal vortex wake," *Journal of experimental Biology* **209**, 2025–2033, June 1, (2006).
13. M. K. Shin, S. I. Kim, S. J. Kim, S. Y. Park, Y. H. Hyun, Y. Lee, K. E. Lee, S.-S. Han, D.-P. Jang, Y.-B. Kim, Z.-H. Cho, I. So, and G. M. Spinks, "Controlled Magnetic Nanofiber Hydrogels by Clustering Ferritin," *Langmuir* **24**, 12107–12111, 2008/11/04 (2008).
14. A. M. Hermansson, "*Marine-Inspired Water-Structured Biomaterials*," ed, 385–395, (2010).
15. M. Kumar, "Radiolytic formation of Ag clusters in aqueous polyvinyl alcohol solution and hydrogel matrix," *Radiation physics and chemistry (Oxford, England : 1993)* **73**, 21–27, (2005).
16. H. Park, K. Park, and W. S. W. Shalaby, *Biodegradable Hydrogels for Drug Delivery*: Taylor & Francis, (1993).
17. T. Miyazaki, K. Yamaoka, J. P. Gong, and Y. Osada, "Hydrogels with Crystalline or Liquid Crystalline Structure," *Macromolecular Rapid Communications* **23**, 447–455, (2002).
18. S. Naficy, H. R. Brown, J. M. Razal, G. M. Spinks, and P. G. Whitten, "Progress Toward Robust Polymer Hydrogels," *Australian Journal of Chemistry* **64**, 1007–1025, (2011).
19. P. Calvert, "Hydrogels for Soft Machines," *Advanced Materials* **21**, 743–756, (2009).
20. Y. Tanaka, J. P. Gong, and Y. Osada, "Novel hydrogels with excellent mechanical performance," *Progress in Polymer Science* **30**, 1–9, (2005).
21. K. Ohara, I. Yamashita, T. Yaegashi, M. Moniwa, M. Yoshimaru, and Y. Uraoka, "Floating Gate Memory with Biomineralized Nanodots Embedded in High-k Gate Dielectric," *Applied physics express* **2**, 095001, (2009).
22. M. K. Shin, G. M. Spinks, S. R. Shin, S. I. Kim, and S. J. Kim, "Nanocomposite Hydrogel with High Toughness for Bioactuators," *Advanced Materials* **21**, 1712–1715, (2009).
23. L. Hsu, C. Weder, and S. J. Rowan, "Stimuli-responsive, mechanically-adaptive polymer nanocomposites," *Journal of Materials Chemistry* **21**, 2812–2822, (2011).
24. S. H. Hyon, W. I. Cha, and Y. Ikada, "Preparation of transparent poly(vinyl alcohol) hydrogel," *Polymer Bulletin* **22**, 119–122, 1989/08/01 (1989).
25. N. A. Peppas and S. R. Stauffer, "Reinforced uncrosslinked poly (vinyl alcohol) gels produced by cyclic freezing-thawing processes: a short review," *Journal of Controlled Release* **16**, 305–310, (1991).
26. L. Mandelkern, "The effect of molecular weight on the crystallization and melting of long-chain molecules," *Journal of Polymer Science Part C: Polymer Symposia* **18**, 51–55, (1967).
27. H. S. Mansur, "Characterization of poly(vinyl alcohol)/poly(ethylene glycol) hydrogels and PVA-derived hybrids by small-angle X-ray scattering and FTIR spectroscopy," *Polymer (Guilford)* **45**, 7193–7202, (2004).
28. F. Yokoyama, I. Masada, K. Shimamura, T. Ikawa, and K. Monobe, "Morphology and structure of highly elastic poly(vinyl alcohol) hydrogel prepared by repeated freezing-and-melting," *Colloid and Polymer Science* **264**, 595–601, 1986/07/01 (1986).
29. ASTM Standard D575-91, 2012 "*Standard Test Methods for Rubber Properties in Compression*", ASTM International, West Conshohocken, PA, (2012). 10.1520/D0575-91R12, www.astm.org
30. ASTM Standard D695-10, 2010, "Standard Test Method for Compressive Properties of Rigid Plastics", ASTM International, West Conshohocken, PA, (2010). 10.1520/D0695-10, www.astm.org
31. A. A. Villanueva, K. B. Joshi, J. B. Blottman, and S. Priya, "A bio-inspired shape memory alloy composite (BISMAC) actuator," *Smart Mater. Struct.* **19**, 025013, (2010).
32. W. M. Megill, "The biomechanics of jellyfish swimming," Ph. D. Dissertation, Department of Zoology, University of British Columbia, (2002).
33. K. B. Joshi, A. Villanueva, C. F. Smith, and S. Priya, "Modeling of Artificial Aurelia aurita Bell Deformation," *Marine Technology Society Journal* **45**, 165–180, (2011).